J. Fluid Mech. (1976), *vol.* 76, *part* 1, *pp.* 113–125
Printed in Great Britain

Rimming flow of liquid in a rotating horizontal cylinder

By K. J. RUSCHAK AND L. E. SCRIVEN

Department of Chemical Engineering and Materials Science,
University of Minnesota, Minneapolis

(Received 27 June 1974 and in revised form 6 November 1975)

Steady two-dimensional flow of Newtonian liquid in a layer around the inside of a rotating horizontal cylinder is analysed as a regular perturbation from rigid-body motion. The equations governing the first perturbation are solved in closed form. Parameter limits are taken in order to elucidate the flow structure and to provide simpler working formulae. The limiting cases are for small Reynolds numbers, which resembles viscous film flow down a curved wall; for large Reynolds numbers, which involves a periodic boundary layer; and for small ratios of average film thickness to cylinder radius. In every case the maximum film thickness occurs in the upper quadrant on the rising side of the cylinder and the minimum thickness is diametrically opposite.

1. Introduction

We consider a special case of the flow of a liquid layer around the inside surface of a rotating horizontal drum or cylinder. Rimming flow, as we shall call it, and closely related rotating flows are encountered in cream separators, in liquid degassers (e.g. debubbling of solutions prior to coating), in some coating operations for pipes and tubes, in rotational moulding and spin casting of plastics, in the casting of molten metal or cement into pipes and columns, and even in the drying of fine powder in a rotating oven.

Rimming flow is a non-trivial example of a steady, two-dimensional, viscous flow with a free surface. The flow domain is bounded, and so the upstream and downstream conditions which are imposed as asymptotic boundary conditions in other film-flow problems are absent. Moreover, the liquid film continuously wets the cylinder surface, and so there are no contact lines. For these reasons the geometry of rimming flow provides one of the simplest frameworks for studying a steady, viscous, free-surface flow and perhaps for analysing some of the instabilities arising in such flows. We also feel that rimming flow is an attractive first problem for the development of numerical methods for free-surface problems, because techniques for locating the free boundary can be studied uncomplicated by asymptotic boundary conditions and the expected singularities at contact lines, where the boundary data are discontinuous (e.g. Richardson 1967; Huh & Scriven 1971; Nickell, Tanner & Caswell 1974).

In the following sections we study rimming flow as a perturbation about rigid-body rotation of the liquid layer at the angular velocity of the drum. There are at least three limiting processes which lead to rigid-body motion: the acceleration

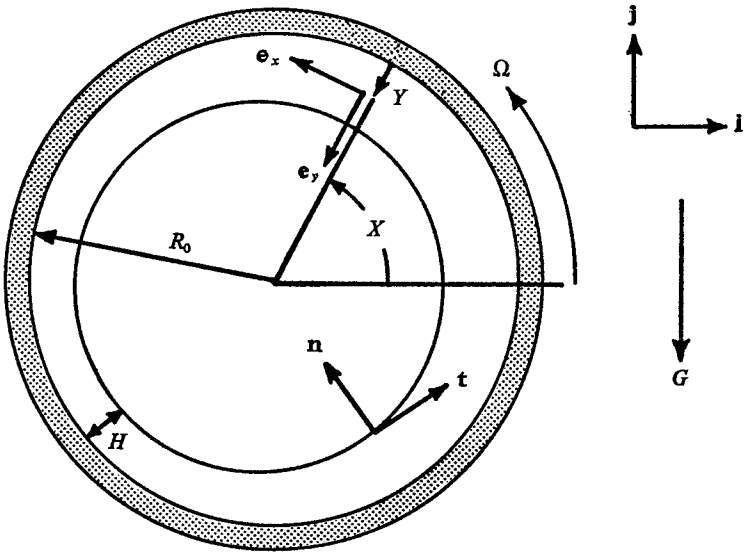

FIGURE 1. Rimming flow.

by gravity tending to zero, the rotation rate of the cylinder tending to infinity, and the radius of the cylinder tending to infinity. We pivot a power-series expansion of a presumed two-dimensional solution to the problem about this limit, and in § 5 solve in closed form the linear elliptic problem generated at first order.

In § 6 we present three limiting forms of our result to make plain the structure of the flow and to provide simpler working formulae. These limiting cases also provide interesting illustrations of some of the principles of slow flow, high-Reynolds-number flow with a viscous boundary layer, and thin-film flow. When the Reynolds number is small, viscous and pressure forces are in balance with the gravitational force. This limiting case was developed by Rao & Throne (1972) in their model of a rotational moulding process under the further restriction that the film is thin. When the Reynolds number is large, a viscous boundary layer lies adjacent to the wall of the drum, as we show. Phillips (1960) obtained the inviscid component of this limiting flow as a step in his treatment of centrifugal waves. Lastly we treat the thin-film limiting case, which has not been previously considered to our knowledge. Observations by Karweit & Corrsin (1975) reveal the complicated structure of rimming flow outside these special cases.

2. Formulation

We consider a horizontal, circular cylinder of inside radius R_0 which rotates at constant angular velocity Ω about its axis: see figure 1. We adopt polar co-ordinates with X the angular azimuthal co-ordinate, Y a radial co-ordinate measured from the inner wall of the cylinder, and $\mathbf{e}_x$ and $\mathbf{e}_y$ the corresponding unit tangent vectors. Position about the axis is $\mathbf{R} = -(R_0 - Y)\,\mathbf{e}_y$. The cylinder is partially filled with Newtonian liquid which is distributed in a layer around the wall. The layer thickness $H(X)$ varies around the cylinder because of the

action of gravity; the local gravitational acceleration is G and the vertical direction is $\mathbf{j}$. Flow in the layer is two-dimensional and steady. The rest of the volume of the cylinder is occupied by relatively rarefied and inviscid gas which exerts negligible viscous traction at the gas/liquid interface and consequently is modelled by a uniform pressure P_a.

The liquid velocity and pressure fields are $\mathbf{V}(\mathbf{R})$ and $P(\mathbf{R})$, respectively. The liquid properties are uniform: density ρ, viscosity μ, kinematic viscosity $\nu \equiv \mu/\rho$ and surface tension σ. The field equations are

$$\left.\begin{aligned} \mathbf{V}.\nabla\mathbf{V} &= -\rho^{-1}\nabla P + \nu\nabla^2\mathbf{V} - G\mathbf{j}, \\ \nabla.\mathbf{V} &= 0. \end{aligned}\right\} \tag{2.1}$$

The customary no-slip boundary condition at the cylinder wall is

$$\mathbf{V} = \Omega R_0 \mathbf{e}_x \quad \text{at} \quad \mathbf{R} = -R_0\mathbf{e}_y. \tag{2.2}$$

The traction balance at the gas/liquid interface gives the boundary condition

$$(P-P_a)\mathbf{n} - \mu[\nabla\mathbf{V} + (\nabla\mathbf{V})^{\mathrm{T}}].\mathbf{n} + \sigma K\mathbf{n} = 0 \quad \text{at} \quad \mathbf{R} = -(R_0-H)\mathbf{e}_y, \tag{2.3}$$

where $\mathbf{n}$ is the unit normal to the interface, directed into the gas, and K is twice the mean curvature of the interface:

$$K = \frac{1 + 2[H_X/(R_0-H)]^2 + H_{XX}/(R_0-H)}{(R_0-H)\{1+[H_X/(R_0-H)]^2\}^{\frac{3}{2}}}. \tag{2.4}$$

The kinematic boundary condition requires that no liquid should cross the interface:

$$\mathbf{n}.\mathbf{V} = 0 \quad \text{at} \quad \mathbf{R} = -(R_0-H)\mathbf{e}_y. \tag{2.5}$$

Finally, it is evident that the solution of (2.1)–(2.5) must be periodic in the angular co-ordinate X with period 2π.

A measure of the amount of liquid in the cylinder is the average film thickness D, which is given by

$$2R_0D - D^2 = \frac{1}{2\pi}\int_0^{2\pi} (2R_0H - H^2)\,dX. \tag{2.6}$$

There are four independent dimensionless groups; convenient choices are

$$g \equiv G/\Omega^2R_0, \quad \mathscr{R} \equiv \Omega D^2/\nu, \quad s \equiv \sigma/\rho\Omega^2R_0^2D, \quad d_r \equiv D/R_0. \tag{2.7}$$

The group g may be considered a dimensionless gravity or an inverse rotational Froude number, $\mathscr{R}$ a Reynolds number, d_r the liquid loading, and s a dimensionless surface tension or Weber number.

Because the velocity field is solenoidal and because

$$\int_0^{2\pi R_0} \mathbf{V}.\mathbf{e}_y\,dS = 0 \quad \text{at} \quad Y = 0, \tag{2.8}$$

where S is the arc length, there exists a stream function ψ, determined up to a constant.

3. Solution in the absence of gravity

When $G = 0$, (2.1)–(2.5) admit a simple solution:

$$\left.\begin{aligned} \mathbf{V} &= \Omega(R_0 - Y)\,\mathbf{e}_x, \\ P - P_a &= \rho\Omega^2[R_0(D-Y) - \tfrac{1}{2}(D^2 - Y^2)] - \sigma/(R_0 - D), \\ H &= D. \end{aligned}\right\} \tag{3.1}$$

This is rigid-body rotation of a film of constant thickness. In the absence of gravity there is no preferred direction, hence the radial symmetry. The pressure gradient balances the centripetal acceleration of the rotating liquid particles. This solution is of little interest in itself. However, a regular perturbation expansion in gravity can be pivoted about the rigid-body motion (3.1). To this end we presume that the limit of the full problem solution as $G \to 0$ is the above solution to the special problem when $G = 0$ and that this limit is approached uniformly.

On physical grounds we expect that the solution with $G = 0$ is the limit of at least two other processes. An estimate of the centripetal acceleration of liquid particles is $\Omega^2 R_0$. When this estimate is large the radial pressure gradient is steep and tends to align constant-density surfaces with the level surfaces of the centripetal acceleration field; thus the liquid film is driven towards an equilibrium state of uniform thickness. The only cause of liquid deformation in a steady state is the gravitational field, and this can be countered by a strong enough centripetal field. Consequently we expect that in the limit as either the angular velocity Ω or the cylinder radius R_0 increases without bound the flow approaches solid-body rotation. Although both limiting processes do lead to the $G = 0$ solution, the mechanisms are quite different. What they have in common is that the influence of gravity is reduced as the relevant parameter increases without bound.

4. Perturbation about rigid-body motion

We introduce the dimensionless position vector

$$\mathbf{r} \equiv \mathbf{R}/R_0 = -(1 - d_r y)\,\mathbf{e}_y, \quad y \equiv Y/D, \quad x \equiv X. \tag{4.1}$$

Dimensionless dependent variables which have non-zero limits as $g \to 0$ are

$$\left.\begin{aligned} \mathbf{v}(\mathbf{r}) &\equiv \mathbf{V}(R_0\mathbf{r})/\Omega R_0, \quad p(\mathbf{r}) \equiv [P(R_0\mathbf{r}) - P_a]/\rho\Omega^2 D R_0, \\ h(x) &\equiv H(x)/D, \quad \kappa(x) \equiv R_0 K(x). \end{aligned}\right\} \tag{4.2}$$

In terms of these the problem (2.1)–(2.6) becomes

$$\mathbf{v}.\nabla\mathbf{v} = -d_r\nabla p + d_r^2\mathscr{R}^{-1}\nabla^2\mathbf{v} - g\mathbf{j}, \tag{4.3a}$$

$$\nabla.\mathbf{v} = 0, \tag{4.3b}$$

$$\mathbf{v} = \mathbf{e}_x \quad \text{at} \quad \mathbf{r} = -\mathbf{e}_y, \tag{4.3c}$$

$$p\mathbf{n} - d_r\mathscr{R}^{-1}[\nabla\mathbf{v} + (\nabla\mathbf{v})^T].\mathbf{n} + s\kappa\mathbf{n} = \mathbf{0}, \quad \mathbf{v}.\mathbf{n} = 0 \quad \text{at} \quad \mathbf{r} = \mathbf{r}_s \equiv -(1 - d_r h)\,\mathbf{e}_y, \tag{4.3d}$$

$$2 - d_r = \frac{1}{2\pi}\int_0^{2\pi} (2h - d_r h^2)\,dx, \tag{4.3e}$$

plus the requirement of periodicity in the azimuthal co-ordinate x. We presume that the dependent variables have power-series expansions in g:

$$\begin{Bmatrix} \mathbf{v} \\ p \\ h \end{Bmatrix} = \sum_{n=0}^{\infty} \begin{Bmatrix} \mathbf{v}^{(n)} \\ p^{(n)} \\ h^{(n)} \end{Bmatrix} g^n. \tag{4.4}$$

The first coefficients are known from (3.1):

$$\mathbf{v}^0 = (1-d_r y)\,\mathbf{e}_x, \quad p^0 = (1-y) - \tfrac{1}{2} d_r (1-y^2) - s/(1-d_r), \quad h^0 = 1. \tag{4.5}$$

Substituting (4.4) into (4.3) generates a sequence of linear problems which determine the rest of the coefficients. In particular the field equations yield

$$\left.\begin{aligned} \mathbf{v}^{(n)}.\nabla\mathbf{v}^0 + \mathbf{v}^0.\nabla\mathbf{v}^{(n)} &= -d_r \nabla p^{(n)} + d_r^2 \mathscr{R}^{-1} \nabla^2 \mathbf{v}^{(n)} + \mathbf{I}_n, \\ \mathbf{I}_1 \equiv -\mathbf{j}, \quad \mathbf{I}_n &= -\sum_{k=1}^{n-1} \mathbf{v}^{(n-k)}.\nabla\mathbf{v}^{(k)}, \quad n > 1, \end{aligned}\right\} \tag{4.6}$$

$$\nabla.\mathbf{v}^{(n)} = 0, \quad n \geqslant 1. \tag{4.7}$$

Direct calculation gives $\nabla\mathbf{v}^0 = \mathbf{e}_x\mathbf{e}_y - \mathbf{e}_y\mathbf{e}_x$. By introducing the stream function $\psi(x,y)$, equation (4.7) is satisfied:

$$\psi = \sum_{n=0}^{\infty} \psi^{(n)} g^n, \quad \mathbf{v}^{(n)} = \psi_y^{(n)}\,\mathbf{e}_x - \frac{d_r}{(1-d_r y)}\,\psi_x^{(n)}\,\mathbf{e}_y \tag{4.8}$$

(subscripts x and y on ψ denote partial derivatives). Substituting $\mathbf{v}^{(n)}$ into the curl of (4.6) yields

$$[\nabla^2\psi^{(n)}]_x = d_r^2 \mathscr{R}^{-1} \nabla^4 \psi^{(n)} + d_r^{-1} (\nabla \times \mathbf{I}_n).\mathbf{k}, \tag{4.9}$$

where $\mathbf{k} \equiv \mathbf{e}_y \times \mathbf{e}_x$. This is the linear inhomogeneous partial differential equation which must be solved at each order.

The boundary conditions at the cylinder wall are, from (4.3),

$$\mathbf{v}^{(n)} = 0 \quad \text{at} \quad \mathbf{r} = -\mathbf{e}_y, \quad n \geqslant 1. \tag{4.10}$$

The g dependence of the interfacial position complicates the introduction of expansions (4.4) into the free-surface boundary conditions. For example, the expansion of dimensionless surface velocity begins

$$\mathbf{v}(\mathbf{r}_s; g) = \mathbf{v}^0(\mathbf{r}_0) + g[d_r h^{(1)} (\mathbf{e}_y.\nabla\mathbf{v}^0) + \mathbf{v}^{(1)}(\mathbf{r}_0)] + O(g^2), \tag{4.11}$$

where $\mathbf{r}_0 \equiv -(1-d_r)\,\mathbf{e}_y$. In substituting such expansions into the traction boundary condition it is helpful to have the normal and tangential components of the latter; from (4.3)

$$\left.\begin{aligned} p - d_r \mathscr{R}^{-1} \mathbf{n}.[\nabla\mathbf{v} + (\nabla\mathbf{v})^T].\mathbf{n} + s\kappa &= 0 \\ \mathbf{n}.[\nabla\mathbf{v} + (\nabla\mathbf{v})^T].\mathbf{t} &= 0 \end{aligned}\right\} \quad \text{on} \quad \mathbf{r} = \mathbf{r}_s, \tag{4.12}$$

where $\mathbf{t}$ is the unit tangent to the interface profile $h(x)$. The interfacial boundary conditions on (4.6) and (4.7) with $n = 1$ now follow: at $\mathbf{r} = \mathbf{r}_0$

$$p^{(1)} - (1-d_r) h^{(1)} - d_r \mathscr{R}^{-1} \mathbf{e}_y.[\nabla\mathbf{v}^{(1)} + (\nabla\mathbf{v}^{(1)})^{\mathrm{T}}].\mathbf{e}_y + s d_r (1-d_r)^{-2} [h_{xx}^{(1)} + h^{(1)}] = 0, \tag{4.13}$$

$$\mathbf{e}_x.[\nabla\mathbf{v}^{(1)} + (\nabla\mathbf{v}^{(1)})^{\mathrm{T}}].\mathbf{e}_y = 0, \quad \mathbf{v}^{(1)}.\mathbf{e}_y = d_r h_x^{(1)}. \tag{4.14), (4.15}$$

Condition (4.3*e*) becomes the integral constraint

$$\int_0^{2\pi} h^{(1)}(x)\,dx = 0. \tag{4.16}$$

5. Solution at first order

When $n = 1$, $\mathbf{I}_1 = -\mathbf{j}$ and so (4.9) is homogeneous:

$$[\nabla^2\psi^{(1)}]_x = d_r^2\mathscr{R}^{-1}\nabla^4\psi^{(1)}. \tag{5.1}$$

The only inhomogeneity in the first-order problem appears in (4.6), which gives $p^{(1)}$. The inhomogeneity is $\mathbf{I}_1 = -\cos x\,\mathbf{e}_x + \sin x\,\mathbf{e}_y$ and this along with the periodicity requirement suggests that the solution has the form

$$\psi^{(1)} = \mathrm{Re}\,[e^{ix}f(y)]. \tag{5.2}$$

Hereafter the real part is understood. From (5.2)

$$\nabla^2\psi^{(1)} = e^{ix}\mathscr{L}f, \quad \mathscr{L}f \equiv d_r^{-2}f_{yy} - [d_r(1-d_r y)]^{-1}f_y - (1-d_r y)^{-2}f, \tag{5.3}$$

whence (5.1) reduces to a fourth-order equation in f:

$$i\mathscr{L}f = d_r^2\mathscr{R}^{-1}\mathscr{L}^2 f. \tag{5.4}$$

This has the general solution

$$f = k_1(1-d_r y) + k_2(1-d_r y)^{-1} + k_3 J_1[\alpha(y)] + k_4 Y_1[\alpha(y)], \tag{5.5}$$

where the k_i's are constants to be chosen later to satisfy the boundary conditions, and $\alpha(y) \equiv (\frac{1}{2}\mathscr{R})^{\frac{1}{2}}(1-i)(1-d_r y)/d_r$. Here J_1 and Y_1 are Bessel functions of order one of the first and second kinds, respectively (Watson 1945, chap. 3).

Before boundary conditions on f can be identified, expressions for $h^{(1)}$ and $p^{(1)}$ in terms of f must be found. Equation (4.6) can be integrated to give $p^{(1)}$ once the complex representations of $\mathbf{v}^{(1)}$ and $\mathbf{I}_1$ have been substituted:

$$p^{(1)} = -e^{ix}\left\{\frac{1-d_r y}{d_r}f_y + 2f - i\frac{1-d_r y}{d_r} + \frac{i}{\mathscr{R}}\left[\frac{1-d_r y}{d_r}f_{yyy} - f_{yy} - \frac{2d_r}{(1-d_r y)}f_y - \frac{2d_r^2}{(1-d_r y)^2}f\right]\right\}. \tag{5.6}$$

An expression for $h^{(1)}$ is found by substituting the complex representation of $\mathbf{v}^{(1)}$ in (4.15), integrating and applying the integral constraint (4.16):

$$h^{(1)} = -f(1)\,e^{ix}/(1-d_r). \tag{5.7}$$

Thus boundary conditions (4.10) and (4.14) become, respectively,

$$f(0) = f_y(0) = 0, \tag{5.8), (5.9}$$

$$f_{yy}(1) + d_r(1-d_r)^{-1}f_y(1) + d_r^2(1-d_r)^{-2}f(1) = 0. \tag{5.10}$$

The remaining condition at $y = 1$ is (4.13). From (5.7), $h^{(1)}_{xx} + h^{(1)} = 0$, which removes the surface-tension term from (4.13). The circular free surface found at

$g = 0$ undergoes a small displacement with respect to the drum at first order but is not distorted. In final form, the boundary condition from (4.13) is

$$f_{yyy}(1) - \frac{d_r}{1-d_r} f_{yy}(1) - \left[\frac{4d_r^2}{(1-d_r)^2} + i\mathscr{R}\right]\left[f_y(1) + \frac{d_r f(1)}{1-d_r}\right] = \mathscr{R}. \tag{5.11}$$

Of the four boundary conditions (5.8)–(5.11), only the last is inhomogeneous. The Reynolds-number term on the right side of (5.11) is directly descended from $\mathbf{I}_1$ in (4.6), and thus the inhomogeneity originates from the presence of gravity.

The four boundary conditions (5.8)–(5.11) are sufficient to determine the constants in the solution (5.5):

$$\left.\begin{aligned} k_1 &= -i(1-d_r)^2/2d_r - k_3 J_1(\alpha_0) - k_4 Y_1(\alpha_0), \\ k_2 &= i(1-d_r)^2/2d_r, \\ k_3 &= [i(1-d_r)/d_r]\,[a_2 - (1-d_r)\,a_4]/[a_1 a_4 - a_2 a_3], \\ k_4 &= [i(1-d_r)/d_r]\,[(1-d_r)\,a_3 - a_1]/[a_1 a_4 - a_2 a_3]. \end{aligned}\right\} \tag{5.12}$$

The new parameters are

$$\left.\begin{aligned} a_1 &\equiv 2J_1(\alpha_0) - \alpha_0 J_0(\alpha_0), & a_3 &\equiv (2 - \tfrac{1}{2}\alpha_1^2) J_1(\alpha_1) - \alpha_1 J_0(\alpha_1), \\ a_2 &\equiv 2Y_1(\alpha_0) - \alpha_0 Y_0(\alpha_0), & a_4 &\equiv (2 - \tfrac{1}{2}\alpha_1^2) Y_1(\alpha_1) - \alpha_1 Y_0(\alpha_1), \\ \alpha_0 &\equiv \alpha(0), & \alpha_1 &\equiv \alpha(1). \end{aligned}\right\} \tag{5.13}$$

This completes the solution for f, from which the stream function $\psi^{(1)}$ and hence $\mathbf{v}^{(1)}$, $p^{(1)}$ and $h^{(1)}$ all follow directly. This solution to the first-order problem is unique. In the next section we examine limiting cases of these expressions in order to illustrate the structure of the solution and to provide simpler working formulae.

6. Limiting cases of rimming flow

The foregoing solution to the first-order problem depends on the two groups $\mathscr{R}$ and d_r. When the Reynolds number $\mathscr{R}$ is small the Bessel functions in (5.5), (5.12) and (5.13) can be replaced by their asymptotic developments for arguments of small modulus (Watson 1945, chap. 3). The outcome of this tedious but straightforward task is

$$\begin{aligned} \mathbf{v}^{(1)}/\mathscr{R} \sim \hat{\mathbf{v}} &= d_r^{-2}\{c_1 + 3c_2(1-d_r y)^2 - c_3(1-d_r y)^{-2} + c_4[1 + \ln(1-d_r y)]\}\cos x\,\mathbf{e}_x \\ &\quad - d_r^{-2}\{c_1 + c_2(1-d_r y)^2 + c_3(1-d_r y)^{-2} + c_4 \ln(1-d_r y)\}\sin x\,\mathbf{e}_y, \qquad (6.1a) \\ p^{(1)} \sim \hat{p} &= d_r^{-1}[(8c_2 - 1)(1-d_r y) - 2c_4(1-d_r y)^{-1}]\sin x, \qquad (6.1b) \\ h^{(1)}/\mathscr{R} \sim \hat{h} &= d_r^{-3}[c_1 + c_2(1-d_r)^2 + c_3(1-d_r)^{-2} + c_4 \ln(1-d_r)]\cos x, \qquad (6.1c) \end{aligned}$$

where, with $c \equiv 1 - d_r$,

$$\left.\begin{aligned} c_1 &\equiv -c^2(1-c^4)/8(1+c^4), & c_3 &\equiv -c^6/8(1+c^4), \\ c_2 &\equiv c^2/8(1+c^4), & c_4 &\equiv -\tfrac{1}{4}c^2. \end{aligned}\right\} \tag{6.2}$$

These results give the departure from solid-body rotation when both g and $\mathscr{R}$ are small. The nature of this departure depends on the relative amount of liquid

in the cylinder, as reflected by the group d_r. The maximum film thickness occurs on the rising side of the drum, at $x = 0$, a matter which is discussed further in § 7.

The limiting form of (4.6) satisfied by the limits $\hat{\mathbf{v}}$ and $\hat{p}$ of the solution at first order shows that this is a slow-flow limit in which viscous and gravitational forces dominate and are balanced by the pressure field:

$$0 = -d_r \nabla \hat{p} + d_r^2 \nabla^2 \hat{\mathbf{v}} - \mathbf{j}. \tag{6.3}$$

This result suggests that the leading terms in the expansion of the problem solution (4.2) in the Reynolds number are closely related to (6.1). Now it is physically reasonable to suppose that rimming flow approaches rigid-body rotation as $\mathscr{R} \to 0$. Viscosity appears only in the denominator of $\mathscr{R}$ and with viscosity increasing without bound the liquid would ultimately be indistinguishable from solid. Thus we presume that the small-Reynolds-number expansions begin

$$\left.\begin{aligned} \mathbf{v} &\sim \mathbf{v}^0 + \mathscr{R}\mathbf{W} + \ldots, \\ p &\sim \pi + \ldots, \\ h &\sim 1 + \mathscr{R} l + \ldots. \end{aligned}\right\} \tag{6.4}$$

It is easily verified from (4.3) that

$$\mathbf{W} = g\hat{\mathbf{v}}, \quad \pi = p^0 + g\hat{p}, \quad l = g\hat{h}. \tag{6.5}$$

On the other hand, when the Reynolds number $\mathscr{R}$ is large the Bessel functions in (5.5), (5.12) and (5.13) can be replaced by their asymptotic developments for arguments of large modulus (Watson 1945, chap. 7). Doing so we first calculate the limit of the first-order solution as $\mathscr{R} \to \infty$ with y fixed ($0 < y \leqslant 1$):

$$\left.\begin{aligned} \mathbf{v}^{(1)} \to \mathbf{v}_i \equiv\ & -\tfrac{1}{2}(1-d_r)^2[1+(1-d_r y)^{-2}]\sin x\,\mathbf{e}_x \\ & -\tfrac{1}{2}(1-d_r)^2[1-(1-d_r y)^{-2}]\cos x\,\mathbf{e}_y, \\ p^{(1)} \to p_i \equiv\ & -d_r^{-1}\{(1-d_r y)+\tfrac{1}{2}(1-d_r)^2[(1-d_r y)-3(1-d_r y)^{-1}]\}\sin x, \\ h^{(1)} \to h_i \equiv\ & -\tfrac{1}{2}d_r^{-1}[(1-d_r)^2-1]\sin x. \end{aligned}\right\} \tag{6.6}$$

This is a flow contribution which is irrotational and which in azimuthal velocity alternately lags behind and runs ahead of solid-body rotation in successive quadrants. In the $\mathbf{v}_i$ field there are no net viscous forces: accelerations, or 'inertia forces', and the force of gravity dominate and are just balanced by the pressure field:

$$\mathbf{v}_i . \nabla \mathbf{v}^0 + \mathbf{v}_0 . \nabla \mathbf{v}_i = -d_r \nabla p_i - \mathbf{j}. \tag{6.7}$$

The maximum film thickness occurs at the top of the cylinder ($x = \frac{1}{2}\pi$), a matter discussed in § 7.

As expected of high-Reynolds-number flow near a solid boundary, the limit (6.6) of the first-order problem is not approached uniformly in the flow domain $0 \leqslant y \leqslant 1$. Indeed, the limit of $\mathbf{v}^{(1)}$ is discontinuous with respect to y; for the limit of $\mathbf{v}^{(1)}$ at the cylinder wall is zero and not what $\mathbf{v}_i$ in (6.6) gives as $y \to 0$. To obtain a limit of the full solution (5.5), (5.12) and (5.13) which retains the structure of the flow field near the cylinder wall it is necessary to introduce a boundary-layer co-ordinate:

$$\tilde{y} \equiv (\tfrac{1}{2}\mathscr{R})^{\frac{1}{2}} y. \tag{6.8}$$

Then as $\mathscr{R}\to\infty$ with $\tilde{y}$ fixed, $y\to 0$ at the rate $(2/\mathscr{R})^{\frac{1}{2}}$. The calculations which produce (6.6) make (6.8) the obvious choice for the boundary-layer variable; alternatively, classical boundary-layer problems suggest the choice (cf. Schlichting 1968, chap. 7)

$$\left.\begin{aligned} u^{(1)} &\to \tilde{u} \equiv -(1-d_r)^2[\sin x + e^{-\tilde{y}}\sin(\tilde{y}-x)],\\ (\tfrac{1}{2}\mathscr{R})^{\frac{1}{2}} v^{(1)} &\to \tilde{v} \equiv d_r(1-d_r)^2\{\tilde{y}\cos x - \tfrac{1}{2}(\sin x+\cos x)\\ &\qquad - \tfrac{1}{2}e^{-\tilde{y}}[\sin(\tilde{y}-x)-\cos(\tilde{y}-x)]\},\\ p^{(1)} &\to \tilde{p} \equiv -(2-d_r)\sin x \end{aligned}\right\} \tag{6.9}$$

in the limit as $\mathscr{R}\to\infty$ with $\tilde{y}$ fixed. Here $u^{(1)}$ and $v^{(1)}$ are the x and y components of $\mathbf{v}^{(1)}$, respectively. The limits $\tilde{u}$ and $\tilde{p}$ satisfy an equation of boundary-layer type:

$$\tilde{u}_x = -d_r\tilde{p}_x + \tfrac{1}{2}\tilde{u}_{\tilde{y}\tilde{y}} - \cos x. \tag{6.10}$$

As usual $\tilde{p}$ does not vary across the boundary layer, and the pressure along the boundary layer can be regarded as imposed by the inviscid flow (6.6). When viewed from the cylinder wall, which is turning with tangential velocity ΩR_0, fluid particles far enough away to be outside the boundary layer appear to oscillate in phase because of the sinusoidal variation in the streamwise component of gravity. Particles inside the boundary layer also appear to oscillate, but owing to viscous damping the fluid layers do not oscillate in phase and the amplitude of the oscillation tends to zero at the wall. In Stokes' second problem (Schlichting 1968, p. 85) a wall executing translatory oscillations gives rise to a comparable boundary layer.

In the last of the limiting cases to be examined here, $d_r\to 0$ and the mean film thickness is much smaller than the film circumference. In this limit the liquid layer behaves like a thin film: azimuthal derivatives of velocity and pressure become much smaller than radial derivatives. With $\beta \equiv (\tfrac{1}{2}\mathscr{R})^{\frac{1}{3}}$ it follows from the results of the previous section that as $d_r\to 0$

$$\begin{aligned} u^{(1)} \sim u^* = {} & -\sin x + (\bar{a}\sin x + \bar{c}\cos x)\sin\beta y\cosh\beta y\\ & - (\bar{a}\cos x - \bar{c}\sin x)\cos\beta y\sinh\beta y + e^{-\beta y}\sin(x-\beta y), \end{aligned} \tag{6.11a}$$

$$\begin{aligned} v^{(1)}/d_r \sim v^* = {} & y\cos x + [(\bar{a}+\bar{c}-1)\sin x - (\bar{a}-\bar{c}+1)\cos x]/2\beta\\ & - (\bar{a}\sin x + \bar{c}\cos x)(\cos\beta y\cosh\beta y + \sin\beta y\sinh\beta y)/2\beta\\ & + (\bar{a}\cos x - \bar{c}\sin x)(\cos\beta y\cosh\beta y - \sin\beta y\sinh\beta y)/2\beta\\ & + e^{-\beta y}[\sin(x-\beta y)+\cos(x-\beta y)]/2\beta, \end{aligned} \tag{6.11b}$$

$$\begin{aligned} p^{(1)} \sim p^* = {} & (3y-2)\sin x - [(\bar{a}-\bar{c}+1)\sin x + (\bar{a}+\bar{c}-1)\cos x]/2\beta\\ & + (\bar{a}\sin x + \bar{c}\cos x)(\cos\beta y\cosh\beta y - \sin\beta y\sinh\beta y)/\beta\\ & + (\bar{a}\cos x - \bar{c}\sin x)(\cos\beta y\cosh\beta y + \sin\beta y\sinh\beta y)/\beta\\ & + \bar{e}^{\beta y}[\sin(x-\beta y) - \cos(x-\beta y)]/\beta, \end{aligned} \tag{6.11c}$$

$$h^{(1)} \sim h^* = \sin x - [(\bar{a}-\bar{c}+1)\sin x + (\bar{a}+\bar{c}-1)\cos x]/2\beta. \tag{6.11d}$$

The coefficients $\bar{a}$ and $\bar{c}$ depend only on $\mathscr{R}$:

$$\bar{a} \equiv e^{-\beta} \frac{\sin\beta\cos\beta\,(\sinh\beta+\cosh\beta)}{\cos^2\beta\cosh^2\beta+\sin^2\beta\sinh^2\beta}, \tag{6.12a}$$

$$\bar{c} \equiv e^{-\beta} \frac{\cos^2\beta\cosh\beta-\sin^2\beta\sinh\beta}{\cos^2\beta\cosh^2\beta+\sin^2\beta\sinh^2\beta}. \tag{6.12b}$$

The equations which the limits u^*, v^*, p^* and h^* satisfy clearly indicate the dominance of radial (cross-film) derivatives; for example the limiting form of the azimuthal component of (4.6) is

$$u^*_x = \mathscr{R}^{-1}u^*_{yy} - \cos x. \tag{6.13}$$

This thin-film flow also has large-Reynolds-number and small-Reynolds-number limits. As $\mathscr{R}\to\infty$ a viscous boundary layer arises within the thin film near the cylinder wall, just as in the high-Reynolds-number limit of the general case. As $\mathscr{R}\to 0$, on the other hand,

$$\left.\begin{aligned} u^* &\sim -\mathscr{R}(y-\tfrac{1}{2}y^2)\cos x,\\ v^* &\sim -\mathscr{R}(\tfrac{1}{2}y^2-\tfrac{1}{6}y^3)\sin x,\\ -p^* &\sim (1-y)\sin x+\mathscr{R}(\tfrac{1}{3}-y^2+\tfrac{1}{3}y^3)\cos x,\\ h^* &\sim \tfrac{1}{3}\mathscr{R}\cos x. \end{aligned}\right\} \tag{6.14}$$

Thus when g, d_r and $\mathscr{R}$ are small enough, the flow at any point x on the cylinder is locally indistinguishable from fully developed film flow on an inclined flat plate which is tangential to the cylinder at x and which translates with the velocity of the cylinder at x.

7. Film thickness: concluding remarks

In steady-state rimming flow the flux of liquid across every ray X = constant must be the same. Hence where the average azimuthal velocity is greatest the film must be thinnest, and where it is least the film must be thickest. At low Reynolds number, fluid acceleration is insignificant and the velocity is least where gravity's component opposing viscous drag by the wall is greatest. That occurs at $X = 0$, i.e. where the ascending cylinder wall has a vertical tangent. Thus, at low Reynolds number, the film is thickest at $X = 0$. For the same sort of reason it is thinnest at $X = \pi$, and it takes on its mean thickness at $X = \frac{1}{2}\pi$ and $X = \frac{3}{2}\pi$. All of this is borne out by formulae (6.1) and (6.14).

At high Reynolds numbers the flow is virtually inviscid outside the thin boundary layer at the cylinder wall. Except in the limit, however, the effect of viscosity is not totally absent, for it is responsible for maintaining the 'inviscid zone' at an average angular velocity Ω. Nevertheless, outside the boundary layer in a steady state, viscosity does not impede the acceleration of fluid particles. The principal pressure gradient is generated by the centripetal field and tends to move fluid particles along circular orbits. Gravity is left free to accelerate and decelerate fluid particles along their orbits, which actually are nearly circular. So gravity decelerates fluid particles along their orbits as they

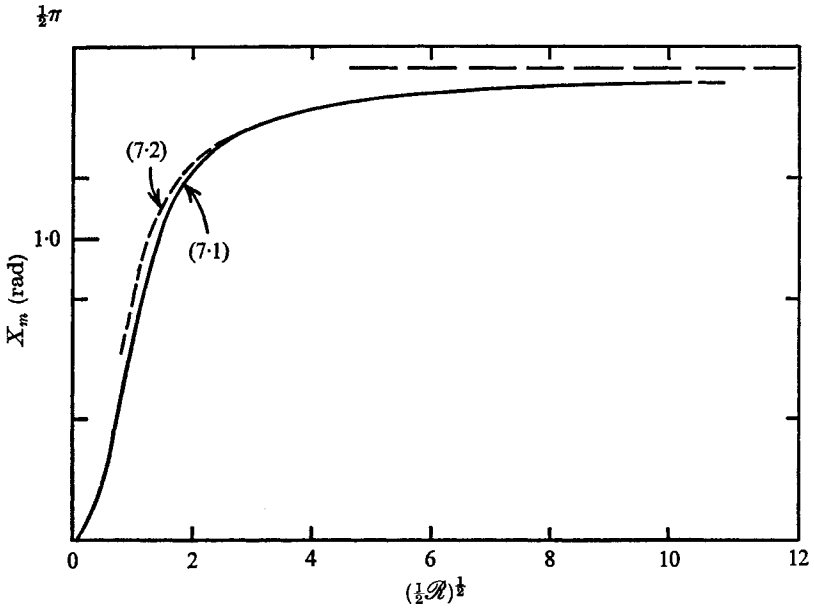

FIGURE 2. Angle (in radians) of maximum film thickness in the limit $d_r \to 0$ when g is small: equation (7.1). The broken curve is (7.2).

travel upwards with the cylinder, and accelerates them as they travel downwards. Thus liquid particles reach minimum azimuthal speed at the top position and so the film is thickest there, i.e. at $X = \frac{1}{2}\pi$. Similarly, it is thinnest at the bottom position $X = \frac{3}{2}\pi$, and it takes on its mean thickness at $X = 0$ and $X = \pi$. This is confirmed by formulae (6.6).

At intermediate Reynolds numbers the location of maximum film thickness is always somewhere in the upper ascending quadrant, $0 < X < \frac{1}{2}\pi$. The location can be estimated for low liquid loadings by working with the limit of H as $d_r \to 0$. Differentiating h^* from (6.11) with respect to x and setting the result to zero, we have

$$\tan X_m = \frac{\bar{a} - \bar{c} + 1 - 2\beta}{\bar{a} + \bar{c} - 1}, \quad d_r \to 0. \tag{7.1}$$

The maxima from (7.1) are plotted in figure 2. From (7.1) it can be shown that

$$\tan X_m \sim (2\mathscr{R})^{\frac{1}{2}} - 1, \quad d_r \to 0, \quad \mathscr{R} \to \infty. \tag{7.2}$$

However, the location of the maximum more generally depends on the liquid loading, as measured by $d_r \equiv D/R_0$ (recall that D is mean layer thickness), as well as on the Reynolds number $\mathscr{R}$. The complete equation to be solved for X_m, the angle of maximum layer thickness, follows from (5.7):

$$\tan X_m = -\operatorname{Im}\{f(1)\}/\operatorname{Re}\{f(1)\}. \tag{7.3}$$

It is no easy matter to compute X_m when $\mathscr{R}$ is near zero, when $\mathscr{R}$ is large or when d_r is small, because small differences between large numbers are required in these cases. However, we have established analytically that (7.1) is indeed the

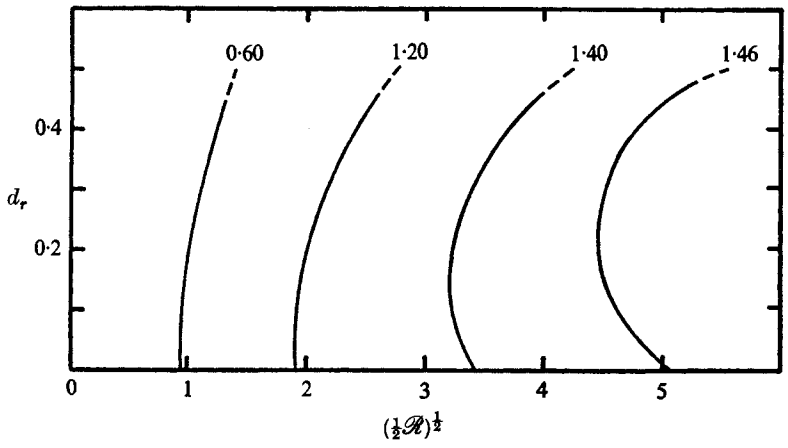

FIGURE 3. Curves indicating constant angle (in radians) of maximum film thickness as a function of liquid loading d_r and Reynolds number $\mathscr{R}$ when g is small: equation (7.3).

limit of (7.3) as $d_r \to 0$ with $\mathscr{R}$ fixed. Moreover the asymptotic behaviour of (7.3) proves to be

$$\tan X_m \sim (\tfrac{1}{2}\mathscr{R})^{\frac{1}{2}} d_r^{-1}[(1-d_r)^{-2}-1]-1, \quad \mathscr{R} \to \infty, \tag{7.4}$$

and the limit of this result as $d_r \to 0$ with $\mathscr{R}$ fixed is (7.2). Figure 3 is based on these facts together with numerical computations, and illustrates the important point that the angle of maximum film thickness is relatively insensitive to liquid loading at modest loadings. Therefore, for a wide range of conditions figure 2 serves to predict X_m accurately as a function of Reynolds number alone. An interesting feature of figure 3 is that *some* pairs $\{X_m, (\frac{1}{2}\mathscr{R})^{\frac{1}{2}}\}$ occur at two separate values of d_r.

It was remarked in § 3 that, although both of the limiting processes $\Omega \to \infty$ and $R_0 \to \infty$ lead to solid-body rotation, the mechanisms are quite different. These mechanisms are now evident. As the cylinder radius $R_0 \to \infty$ when all other parameters are fixed, both $g \to 0$ and $d_r \to 0$, and consequently solid-body rotation is approached through the thin-film limiting case. On the other hand, as the angular velocity $\Omega \to \infty$, all else being fixed, $g \to 0$ and $\mathscr{R} \to \infty$, and as a result solid-body rotation is approached through the limiting case of a viscous boundary layer.

This research was supported by a grant from the National Science Foundation. Professor R. L. Cerro brought rimming flow to our attention, and his numerical simulation of the thin-film case stimulated the present analysis.

REFERENCES

HUH, C. & SCRIVEN, L. E. 1971 Hydrodynamic model of steady movement of a solid/liquid/fluid contact line. *J. Colloid Interface Sci.* **35**, 85–101.

KARWEIT, M. J. & CORRSIN, S. 1975 Observation of cellular patterns in a partly filled, horizontal, rotating cylinder. *Phys. Fluids*, **18**, 111–112.

NICKELL, R. E., TANNER, R. I. & CASWELL, B. 1974 The solution of viscous incompressible jet and free-surface flows using finite-element methods. *J. Fluid Mech.* **65**, 189–206.

PHILLIPS, O. M. 1960 Centrifugal waves. *J. Fluid Mech.* **7**, 340–352.

RAO, M. A. & THRONE, J. L. 1972 Principles of rotational molding. *Polymer Engng Sci.* **12**, 237–64.

RICHARDSON, S. 1967 Slow viscous flows with free surfaces. Ph.D. dissertation, University of Cambridge.

SCHLICHTING, H. 1968 *Boundary Layer Theory*, 6th edn. McGraw-Hill.

WATSON, G. N. 1945 *A Treatise on the Theory of Bessel Functions*. Cambridge University Press.